Cerenkov line-like radiation, the extended and improved formulae system

J.-H. You[1], Y.D. Xu[1], D.B. Liu[1], J.R. Shi[2], and G.X. Jin[1]

[1] Department of Applied Physics, Shanghai Jiao Tong University, Shanghai, 200030, P.R. China
[2] Beijing Astronomical Observatory, Chinese Academy of Sciences, Beijing 100012, P.R. China
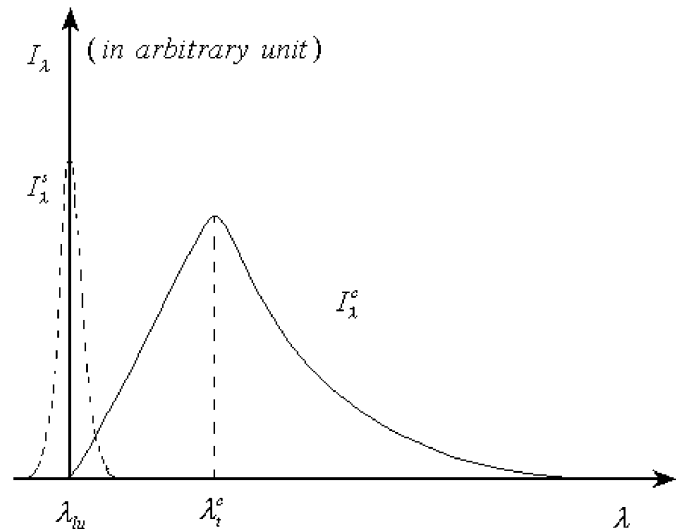
Abstract. You & Cheng (1980) argued that, for relativistic electrons moving through a dense gas, the Cerenkov effect will produce peculiar atomic and/or molecular emission lines–Cerenkov lines. They presented a series of formulae to describe the new line-mechanism. Elegant experimental confirmation has been obtained by Xu. et al. in the laboratory which definitely verified the existence of Cerenkov lines. Owing to the potential importance in high energy astrophysics, in this paper we give a more detailed physical discussion of the emission mechanisms and improve the previous formulae system into a form which is more convenient for astrophysical application. Specifically, the extended formulae in this paper can be applied to other species of atoms and/or ions rather than hydrogen as in the previous paper, and also to X-ray astronomy. They can also be used for the calculation of a nonuniform plane-parallel slab of the emissive gas.

Fig. 1. Comparison of the schematic profiles of the Cerenkov line $I_\lambda^c \sim \lambda$ and the normal line by spontaneous transition process $I_\lambda^s \sim \lambda$. The former has been red-shifted and has asymmetry and large linewidth.

1. Introduction

Early in the 1980's, You & Cheng (1980) mentioned that, when relativistic electrons pass through a dense gas region, the radiation produced by the Cerenkov effect will be concentrated into a narrow waveband $\Delta\lambda$, very near to the intrinsic atomic or molecular wavelength position λ_{lu} (u, l denote the corresponding upper and lower levels respectively). Therefore it looks more like an atomic emission line (for gas composed of atoms) and/or molecular line (for molecular gas), rather than a continuum. They called it the "Cerenkov Emission Line". Later, they presented a series of formulae to describe the properties of the peculiar Cerenkov line (You et al. 1984, 1986). Elegant experimental confirmation of Cerenkov line in O_2, Br_2 gas, and Na vapor using a ^{90}Sr β-ray source has been obtained in the laboratory (Xu et al. 1981, 1988, 1989). By use of the fast coincidence technique, they found the line emission at the expected directions,

Send offprint requests to: J.-H. You (jhyou@online.sh.cn)

wavelengths and plane of polarization. It has been emphasized (You et al. 1986) that the Cerenkov emission line is not a real line in the precise meaning due to the following features: (I) it is rather broad, for a dense gas with $N_H \simeq 10^{15}\text{cm}^{-3}, T \simeq 10^4\text{K}$, the calculated linewidth of Cerenkov $L_{y\alpha}$ is $\Delta\lambda \simeq$ 1–10 Å; (II) generally, the line profile is asymmetric, being steep on the blue side and flat on the red side; (III) its peak is not precisely at λ_{lu}, but slightly red-shifted, we call this the "Cerenkov line redshift", so as to distinguish it from other types of redshift mechanisms (Doppler, gravitational, Compton etc.); (IV) it is polarized if the relativistic electrons have an anisotropic velocity distribution.

The schematic profile of the Cerenkov line $I_\lambda^c \sim \lambda$ is shown in Fig. 1, where the profile of the normal emission line $I_\lambda^s \sim \lambda$ produced by a spontaneous transition process (recombination-cascade and/or collisional excitation) is also presented for comparison.

Here, we emphasize the special importance of point (III). It is the Cerenkov line-redshift which strengthens the emergent intensity of the Cerenkov emission line. The reason is easy to understand. For an optically thick dense gas, the emergent line

flux is determined both by the emission and the absorption. The absorption mechanisms for the normal lines (recombination-cascade and collisional excitation) and for the Cerenkov lines are extremely different. The line-intensity I^s of a normal line is greatly weakened by the large resonance absorption $k_{lu}(\lambda_{lu})$ due to the fact that the normal line is located at the position of the intrinsic wavelength $\lambda = \lambda_{lu}$ (see Fig. 1). where $k_{lu}(\lambda_{lu})$ is very large, $k_{lu}(\lambda_{lu}) \rightarrow \infty$ (In the extreme case of a very dense gas, the emergent flux has a continuum with black body spectrum, and the line intensity $I^s \simeq 0$). However, the Cerenkov line, located at $\lambda > \lambda_{lu}$ because of the small "Cerenkov line-redshift" (generally, $\Delta Z^c \equiv \frac{\Delta \lambda_p}{\lambda_{lu}} \simeq 10^{-3}$, or the apparent "velocity" V a few hundred km s^{-1}) can avoid the strong line absorption k_{lu} because $k_{lu}(\lambda > \lambda_{lu}) \rightarrow 0$. Therefore, the Cerenkov line intensity I^c is only affected by a very small photoelectric absorption k_{bf}, and $k_{bf} \ll k_{lu}(\lambda_{lu})$, which means that the photons of the Cerenkov line can easily escape from deep inside a dense gas cloud. The depth scale is $L \simeq 1/k_{bf} \gg 1/k_{lu}(\lambda_{lu})$, causing a strong emergent intensity I^c only if the density of fast electrons N_e is large enough. In other words, the dense gas appears to be more "transparent" for the Cerenkov lines than for the normal lines, which makes it possible for the Cerenkov line mechanism to dominate over the normal line emission in some physical situations.

Such a new line emission mechanism has a potential importance for high energy astrophysics, particularly in X-ray astronomy. Solar flares, QSOs and other AGNs etc. would be the first candidates. It is known that there definitely exist abundant relativistic electrons and dense gas regions in these objects, which provide the right conditions for producing the Cerenkov line-like radiation. You et al. tried to explain a series of particular observation characteristics of the broad lines of QSOs and Seyfert1 galaxies by use of the new mechanism. Moderate successes have been obtained, at least qualitatively, e.g. (1) the anomalous line-intensity ratios (the steep Balmer decrement, the small ratio $L_{y\alpha}/H_\beta$, etc.)(You & Cheng 1987); (2) the small redshift and red-asymmetry of the broad H_β line with respect to CIV $\lambda 1549$ (Cheng et al. 1990); (3) the different lag times τ of the high-ionized lines, e.g. CIV and the low-ionized lines, e.g. MgII $\lambda 2798$, H_β, with respect to the flare of the continuum from the central source. The progress in the study of QSOs and AGNs in recent years, both in theories and observations mean that we can now make qualitative statements on the contribution of the Cerenkov line mechanism to the broad lines of AGNs. The latest observations which seem favorable to that Cerenkov line mechanism were provided by ASCA observations of Seyfert1 galaxies, which show an iron K_α broad line with a markedly asymmetric profiles (Tanaka, et al. 1995, K. Nandra, et al. 1997, Turner et al. 1997). The very steep blue side and strong red wing of broad K_α line might be indicative of Cerenkov line which encourages us to reexamine and improve the formulae system of the Cerenkov line mechanism given in our previous papers (You et al. 1984, 1986), in a form which is convenient for astrophysical applications. In particular, we hope that the extended formulae can be applied to other species of multi-electron complex atoms and/or ions rather than hydrogen or hydrogenic atoms as

in the previous paper, which are important for the study of the broad lines of AGNs, particularly in the X-ray band. Another extension concerns the discussion on the Cerenkov line redshift in Sect. 2, where we give a generalized formula of the Cerenkov line redshift and its simplified forms in the limiting cases of high and low gas-densities respectively. We find that the conclusion of asymmetry of the line-profile is correct only for a dense gas whose density is larger than a given critical value N^{cr}. When $N \ll N^{cr}$, the profile becomes more symmetric. Finally, our new formulae system is extended to the case of a non-uniform plane-parallel slab of emission gas ($N = N(s), T = T(s)$ etc., where s is the inner distance to the surface of the slab), which is also important in practice.

2. Basic formulae

The CGSE system of units will be used throughout. This means, in particular, that all wavelengths in the following formulae will be in centimeters rather than Å. The photon energy will be in ergs rather than KeV.

2.1. The refractive index n_λ and the extinction coefficient κ_λ

2.1.1. Formulae for hydrogen or hydrogen-like gas

The essential point of the calculation of the spectrum of Cerenkov radiation is the evaluation of the refractive index n of the gaseous medium. This is easy to understand qualitatively from the necessary condition for producing Cerenkov radiation, $V > c/n_\lambda$. At a given wavelength λ, the larger the index n, the easier the condition $V > c/n_\lambda$ to be satisfied, and the stronger the Cerenkov radiation at λ will be. Therefore, in order to get the theoretical spectrum of the Cerenkov radiation, it is necessary to calculate the refractive index n_λ and its dependence on λ, i.e. the dispersion curve $n_\lambda \sim \lambda$. For a gaseous medium, the calculation of the $n_\lambda \sim \lambda$ curve is easy to do. Because our main interest is in the calculation of n_λ in the vicinity of λ_{lu}, we must use the rigorous formula:

$$\frac{\tilde{n}^2 - 1}{\tilde{n}^2 + 2} = \frac{4\pi}{3} N\alpha, \tag{1}$$

where

$$\tilde{n} = n - i\kappa \tag{2}$$

$\tilde{n}$ is the complex refractive index, the real part n is the refractive index of the gas, the imaginary part κ is the extinction coefficient. N is the number density of the atoms, and α is the polarizability per atom. When the atoms are distributed over various energy levels with density N_a in level a, $N\alpha$ will be replaced by $\sum_a N_a \alpha_a$. According to quantum theory, the atomic polarizability per atom in level a is given as (e.g. Handbook of Physics ed. Condon and Odishaw, 1958):

$$\alpha_a(\omega) = \frac{e^2}{m} \sum_{a \neq b} \frac{f_{ab}}{(\omega_{ab}^2 - \omega^2) + i\Gamma_{ab}\omega} \tag{3}$$

where e and m are the charge and the mass of an electron, f_{ab} and Γ_{ab} are the oscillation strength and the damping constant

for the atomic line of frequency ω_{ab}. Substituting Eq. (3) into Eq. (1), we get:

$$N\alpha = \sum_a N_a \alpha_a$$
$$= \sum_a N_a \sum_{b \neq a} \frac{e^2}{2\pi m} \frac{f_{ab}}{2\pi(\nu_{ab}^2 - \nu^2) + i\Gamma_{ab}\nu} \tag{4}$$

Because we are concerned with the neighborhood of a given atomic line λ_{lu}, or the intrinsic frequency ν_{lu}, $\nu \simeq \nu_{lu}$ (the subscripts u and l denote the upper and lower-levels corresponding to the intrinsic frequency ν_{lu}), it follows that we only need to keep the two largest terms in the above summation, Eq. (4) becomes:

$$N\alpha \simeq N_l \alpha_{lu} + N_u \alpha_{ul} \tag{5}$$

where

$$\alpha_{lu} = \frac{e^2}{2\pi m} \frac{f_{lu}}{2\pi(\nu_{lu}^2 - \nu^2) + i\Gamma_{lu}\nu} \tag{6}$$

and α_{ul} is obtained from Eq. (6) by replacing f_{lu} by f_{ul}. Note that f_{lu} and f_{ul} represent the absorption and emission oscillation strengths respectively, corresponding to the pair of energy levels (l, u) of a given atom. Therefore, f_{lu} and f_{ul} are related to each other through the statistical weights g_l and g_u, $g_l f_{lu} = -g_u f_{ul}$. The absorption oscillation strength f_{lu} is related with Einstein's spontaneous emission coefficient A_{ul} as (Bethe & Salpeter 1957):

$$f_{lu} = \frac{mc^3}{8\pi^2 e^2 \nu_{lu}^2} \left(\frac{g_u}{g_l}\right) A_{ul} \tag{7}$$

and the damping constant Γ_{lu} is also related with Einstein's coefficient A_{ul} as:

$$\Gamma_{lu} = \Gamma_l + \Gamma_u = \sum_{i(<l)} A_{li} + \sum_{j(<u)} A_{uj} \tag{8}$$

Using these relations, Eq. (1) becomes:

$$\frac{\tilde{n}^2 - 1}{\tilde{n}^2 + 2} = \frac{b}{z + ig} \tag{9}$$

with

$$b \equiv \frac{c^3}{12\pi^2} \nu_{lu}^{-2} A_{ul} g_u \left(\frac{N_l}{g_l} - \frac{N_u}{g_u}\right)$$
$$z \equiv 2\pi \left(\nu_{lu}^2 - \nu^2\right) \tag{10}$$
$$g \equiv \Gamma_{lu}\nu$$

From Eq. (9) and Eq. (2), we obtain the refractive index n_ν and the extinction coefficient κ_ν as:

$$n_\nu^2 = \left[\left(A^2 + 9b^2 g^2\right)^{1/2} + A\right]/2B$$

$$\kappa_\nu^2 = \left[\left(A^2 + 9b^2 g^2\right)^{1/2} - A\right]/2B \tag{11}$$

where

$$A \equiv (z + 2b)(z - b) + g^2$$

$$B \equiv (z - b)^2 + g^2$$

Eq. (11) is the $n_\nu^2 \sim \nu$ dispersion formula, which we need. The $n_\nu^2 \sim \nu$ dispersion curve can be easily obtained by the digital calculation by use of Eq. (11).

However, as a good approximation, Eq. (11) can be replaced by a simple analytic formula as follows. For convenience in comparing with the observations, it is better to replace the frequency ν in Eq. (9) by wavelength λ, let $\Delta\lambda \equiv \lambda - \lambda_{lu}$ represent the wavelength displacement, and let

$$y \equiv \frac{\lambda - \lambda_{lu}}{\lambda_{lu}} = \frac{\Delta\lambda}{\lambda_{lu}} \tag{12}$$

denote the fractional displacement, $y \ll 1$ because we are always interested in the calculation in the neighborhood of λ_{lu}, $\lambda \simeq \lambda_{lu}$. Therefore the small dimensionless quantity y will be very useful in theoretical analysis (e.g. the expansion series by use of the small quantity y). Replacing $\nu \to \lambda$ in Eq. (11), $\nu = c/\lambda = c\lambda_{lu}^{-1}(1 + y)^{-1}$, and $\nu_{lu} = c\lambda_{lu}^{-1}$. Substituting this into Eq. (10) and Eq. (11), and keeping only the terms of the lowest order in y, we get:

$$b = \frac{c}{12\pi^2} \lambda_{lu}^2 A_{ul} g_u \left(\frac{N_l}{g_l} - \frac{N_u}{g_u}\right)$$

$$z = 4\pi c^2 \lambda_{lu}^{-2} y \tag{13}$$

$$g = c\lambda_{lu}^{-1} \Gamma_{lu}$$

Therefore, among the three quantities b, g and z, only z is $\Delta\lambda$-dependent. Because the Cerenkov line emission is not located in the exact position $\lambda = \lambda_{lu}$, it has a small redshift, so y is not an indefinitely small quantity ($y \nrightarrow 0$, in fact, at $y = 0$, i.e. $\lambda = \lambda_{lu}$, the Cerenkov radiation disappears). In the actually effective range of y, we always have:

$$g \ll z, \quad b \ll z \tag{14}$$

For example, for $Ly\alpha$, $l = 1, u = 2, \lambda_{12} = 1.216 \times 10^{-5}$cm, $\Gamma_{12} = A_{21} = 6.25 \times 10^8$sec^{-1}. Inserting these value in Eq. (13), we find that $g \ll z$ whenever $\Delta\lambda \geq 2.0 \times 10^{-4}$ Å (equivalently, $y \geq 10^{-7}$). On the other hand, under ordinary physical conditions, we can safely assume $N_2 \ll N_1 \sim N$. Then even for N_1 as high as $N_1 \simeq N \simeq 10^{17}$cm^{-3}, $b \ll z$ will be true whenever $\Delta\lambda$ is greater than 1.1×10^{-3}Å (or $y \geq 10^{-6}$). A smaller N will give a still lower limit of $\Delta\lambda$. Therefore, the inequalities (14) always hold in the actually effective Cerenkov line-width ($\Delta\lambda \simeq 1$–10 Å). For the other lines, we obtain the same conclusion (14), under similar considerations. Thus we need only retain the terms of the lowest order of the small quantities g/z and b/z in Eq. (11), and we obtain:

$$n^2 - 1 \simeq 3\frac{b}{z}$$
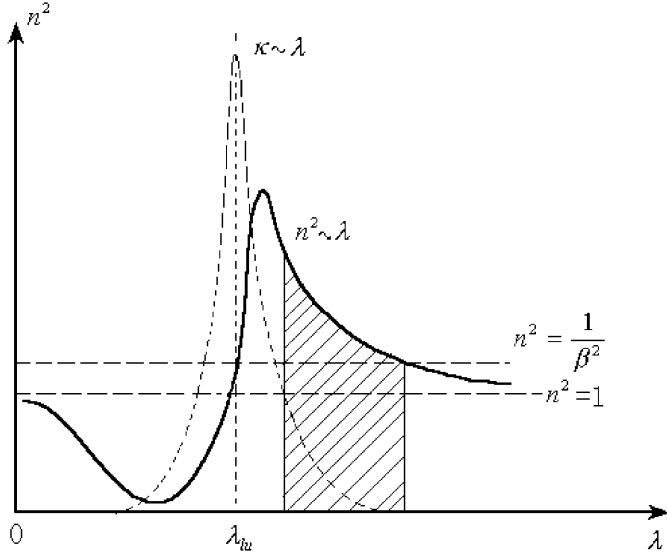
Fig. 2. Relation between refractive index n and wavelength λ, and relation between extinction coefficient and wavelength. The Cerenkov radiation survives in the shaded narrow region.

$$\kappa \simeq \frac{2}{3}\left(\frac{b}{z}\right)\left(\frac{g}{z}\right) \tag{15}$$

Substituting Eq. (13) into Eq. (15), finally we have the simplified approximate formulae:

$$n^2 - 1 = \frac{1}{16\pi^3 c}\lambda_{lu}^4 A_{ul} g_u \left(\frac{N_l}{g_l} - \frac{N_u}{g_u}\right) y^{-1}$$

$$\kappa = \frac{1}{128\pi^4 c^2}\lambda_{lu}^5 \Gamma_{lu} A_{ul} g_u \left(\frac{N_l}{g_l} - \frac{N_u}{g_u}\right) y^{-2} \tag{16}$$

Eqs. (16) are the approximate analytic formulae for n and κ respectively. From Eq. (16) we see that n_λ varies as $(n^2-1) \propto y^{-1} \propto \Delta\lambda^{-1}$. We shall see below that the Cerenkov spectral emissivity varies approximately as $J_\lambda \propto n^2-1$, so $J_\lambda \propto \Delta\lambda^{-1}$. However, the absorption varies as $\kappa_\lambda \propto y^{-2} \propto \Delta\lambda^{-2}$, i.e. the absorption decreases with $\Delta\lambda$ more rapidly than the emissivity. That is why we have a net Cerenkov radiation at the position $\lambda = \lambda_{lu} + \Delta\lambda$, if $\Delta\lambda$ is not approaching to zero.

The calculated $n_\lambda \sim \lambda$ and $\kappa_\lambda \sim \lambda$ curves are shown in Fig. 2. The shaded region (in Fig. 2) represents a narrow waveband $\Delta\lambda$, very near to the position of intrinsic wavelength λ_{lu}, but with small redshift, where the extinction $\kappa_\lambda \simeq 0$, and the net Cerenkov radiation survives. The waveband $\Delta\lambda$ is so narrow(e.g. a few Å), that looks more like a line-emission, rather than a continuum.

2.1.2. Extended formulae for gas of complex atoms(ions) in optical waveband

We emphasize that our derivation from Eq. (4) to Eq. (16) is limited to gas composed of hydrogen and/or hydrogen-like atoms(ions), e.g. Na, He^+, Fe^{+25}, etc. However, a necessary extention to other multi-electron atoms (ions) can easily be done

when we notice that Eq. (3) represents the contribution of an electron lying in the atomic energy level a to the atomic polarizability α. Therefore, for a given emission line of a given multi-electron atom with frequency ν_{lu}, the quantity $N\alpha$ in Eq. (1) and (5) has to be replaced by $N(S_l\alpha_{lu} + S_u\alpha_{ul})$, i.e.

$$N\alpha \simeq N_l\alpha_{lu} + N_u\alpha_{ul} \Longrightarrow N(S_l\alpha_{lu} + S_u\alpha_{ul}) \quad (5') \tag{5'}$$

where N is the number density of complex atoms. S_l (or S_u) represents the actual occupation number of the electrons at the lower level l (or upper level u) of complex atom. Obviously we have

$$S_l \le g_l \quad \text{and} \quad S_u \le g_u$$

where g_l and g_u are the degeneracy of level l and u respectively. From Eq. (1), (5') and equality $g_l f_{lu} = -g_u f_{ul}$, it is easy to see that, if the levels (l, u) have been fully occupied by electrons ('closed shell'), i.e. $S_l = g_l$ and $S_u = g_u$, then we have $N\alpha = 0$, thus $\tilde{n}_\nu = n_\nu - i\kappa_\nu = 1$. In other words, for the multi-electron complex atoms, the Cerenkov line-like emission related to frequency ν_{lu} can occur only when the upper and/or lower levels (l, u) are not fully occupied, i.e. $S_l < g_l$, and/or $S_u < g_u$[1]. In this case, the formulae for quantities Z and g in Eq. (9) are same as in Eq. (10), but the representation of quantity b has to be changed. When $N_l\alpha_{lu} + N_u\alpha_{ul}$ is replaced by $N(S_l\alpha_{lu} + S_u\alpha_{ul})$, we obtain

$$b \equiv \frac{c^3}{12\pi^2}\nu_{lu}^{-2}A_{ul}g_uN\left(\frac{S_l}{g_l} - \frac{S_u}{g_u}\right) \tag{10'}$$

or

$$b \equiv \frac{c}{12\pi^2}\lambda_{lu}^2 A_{ul}g_uN\left(\frac{S_l}{g_l} - \frac{S_u}{g_u}\right) \tag{13'}$$

Thus the final forms of the Eq. (16) for gas composed of multi-electron complex atoms (ions) become

$$n^2 - 1 = \frac{1}{16\pi^3 c}\lambda_{lu}^4 A_{ul}g_uN\left(\frac{S_l}{g_l} - \frac{S_u}{g_u}\right)y^{-1}$$

$$\kappa_\lambda = \frac{1}{128\pi^4 c^2}\lambda_{lu}^5 \Gamma_{lu} A_{ul}g_uN\left(\frac{S_l}{g_l} - \frac{S_u}{g_u}\right)y^{-2} \tag{16'}$$

In the following sections of this paper, all formulae from Eq. (17) to Eq. (42) are used for hydrogen and hydrogen-like gas both for simplicity and practicality because hydrogen is the most abundant element in the cosmological plasmas. However, most of these equations are valid for the multi-electron complex atoms only if the following replacement is made:

$$\left(\frac{N_l}{g_l} - \frac{N_u}{g_u}\right) \Longrightarrow N\left(\frac{S_l}{g_l} - \frac{S_u}{g_u}\right) \tag{5'}$$

---

[1] This is possible for high temperature cosmological plasmas, where the high ionized ions exists, e.g. for a plasma with $T \simeq 2\text{–}3\times10^6 K$, the most abundant ion-species of iron is Fe^{+16} for which $S_1 = 2 = g_1$, $S_2 = 8 = g_2$, but $S_3 = 0 < g_3$. If $T \simeq 10^7 K$, both the most abundant and averaged species of ironions is Fe^{+19}, for which $S_1 = 2 = g_1$, and $\overline{S_2} \simeq 5 < g_2$.

2.1.3. Extended formulae for complex atoms(ions) gas in the X-ray waveband

Another important extension, which we would like to emphasize in this paper, is related to the possible application of Cerenkov line-like emission in X-ray astronomy because the waveband of some Cerenkov lines of complex atoms (ions), particularly the heavy elements, is in the X-ray range. A possible application of the Cerenkov line mechanism in the X-ray band may be a new explanation for the origin of the broad $K_\alpha \sim 6.4$KeV line of Fe ions observed in Seyfert AGNs in recent years. For convenience in comparing with the observations in the X-ray waveband, it is better to replace the wavelength λ in the formulae given above by the frequency ν, or equivalently, by the photon energy $\epsilon = h\nu$. This is easy to do without any remarkable changes in above formulae. We notice that the dimensionless small quantity y in Eq. (12) can also be written as

$$y \equiv \frac{\lambda - \lambda_{lu}}{\lambda_{lu}} \equiv \frac{\Delta\lambda}{\lambda_{lu}} = -\frac{\Delta\nu}{\nu_{lu}} = -\frac{\Delta\epsilon}{\epsilon_{lu}} \tag{12'}$$

where $\epsilon_{lu} \equiv h\nu_{lu} = \epsilon_u - \epsilon_l$ represents the energy difference of the upper and lower levels (u, l), and $-\Delta\epsilon = h\nu_{lu} - h\nu = \epsilon_{lu} - \epsilon$. i.e. the small quantity y also represents the fractional displacement of the frequency or photon-energy. Inserting Eq. (12') into the equations given above we obtain the following formulae which are suitable to the application to X-ray astronomy:

$$n_\nu^2 - 1 = \frac{c^3 h^4}{16\pi^3} \epsilon_{lu}^{-4} A_{ul} g_u N \left(\frac{S_l}{g_l} - \frac{S_u}{g_u} \right) y^{-1}$$

$$\kappa_\nu = \frac{c^3 h^4}{128\pi^4} \epsilon_{lu}^{-5} \Gamma_{lu} A_{ul} g_u N \left(\frac{S_l}{g_l} - \frac{S_u}{g_u} \right) y^{-2} \tag{16''}$$

2.2. The Cerenkov spectral emissivity $J_\lambda^c (J_y^c)$ and the line width $\Delta\lambda_{\lim}^c (y_{\lim})$

2.2.1. Formulae for hydrogen or hydrogen-like gas

The Cerenkov spectral emissivity can be derived from the dispersion curve $n_\lambda \sim \lambda$ given above. It is known from the theory of Cerenkov radiation that the power emitted in a frequency interval $(\nu, \nu + d\nu)$ by an electron moving with velocity $(\beta = V/c)$ is $P_\nu d\nu = (4\pi^2 e^2 \beta\nu/c) \left(1 - \frac{1}{n_\nu^2 \beta^2}\right) d\nu$. Let $N(\gamma)d\gamma$ be the number density of fast electrons in the energy interval $(\gamma, \gamma + d\gamma)$, ($\gamma = \frac{1}{\sqrt{1-\beta^2}} = mc^2/m_0 c^2$ is the Lorentz factor, which represents the dimensionless energy of the electron), then the power emitted in interval $(\nu, \nu + d\nu)$ by these electrons is $N(\gamma)d\gamma P_\nu d\nu$. For an isotropic velocity distribution of the relativistic electrons as in normal astrophysical conditions, the Cerenkov radiation will also be isotropic(the definite angular distribution of the Cerenkov emission disappears when the relativistic electrons have an isotropic distribution of velocities). Hence, the spectral emissivity per unit volume and unit solid angle is:

$$J_\nu^c d\nu = \frac{1}{4\pi} \int_{\gamma_1}^{\gamma_2} N(\gamma)d\gamma P_\nu d\nu$$

$$= \frac{\pi e^2}{c} \nu d\nu \int_{\gamma_1}^{\gamma_2} N(\gamma)d\gamma \beta \left(1 - \frac{1}{n^2\beta^2}\right) \tag{17}$$

where, γ_1, γ_2 are the lower and upper limit of the energy spectrum of the relativistic electrons respectively. For the relativistic electrons, we always have $\beta \simeq 1$, $\gamma \gg 1$, so $\beta^{-2} \simeq 1 + \gamma^{-2}$, $\beta \simeq 1 - \frac{1}{2}\gamma^{-2}$. Also we notice that in the actual effective emission range, the actual refractive index n of a gas is not far from unity, $n \sim 1$ (see Eq. (16)). Therefore:

$$\int_{\gamma_1}^{\gamma_2} N(\gamma) \left(1 - \frac{1}{n^2\beta^2}\right) \beta d\gamma$$

$$\simeq \int_{\gamma_1}^{\gamma_2} \left(n^2 - 1 - \gamma^{-2}\right) N(\gamma)d\gamma$$

$$\simeq \left(n^2 - 1 - \gamma_c^{-2}\right) N_e$$

where, $N_e \equiv \int_{\gamma_1}^{\gamma_2} N(\gamma)d\gamma$ is the density of the relativistic electrons, and γ_c is the characteristic energy of the electrons (or the typical energy) in a given source. The definition of γ_c is $\int_{\gamma_1}^{\gamma_2} \gamma^{-2} N(\gamma)d\gamma \equiv \gamma_c^{-2} N_e$, so $\gamma_1 < \gamma_c < \gamma_2$. Hence:

$$J_\nu^c d\nu \simeq \frac{\pi e^2}{c} N_e \nu \left(n^2 - 1 - \gamma_c^{-2}\right) d\nu \tag{18}$$

Replacing ν to λ or y, we have $J_\nu^c d\nu = J_\epsilon^c d\epsilon = J_\lambda^c d\lambda = J_y^c dy$ and $dy = \lambda_{lu}^{-1} d\lambda = \lambda_{lu}^{-1}(-c\nu^{-2}d\nu)$. Therefore:

$$J_y^c dy = \pi c e^2 N_e \lambda_{lu}^{-2} \left(n^2 - 1 - \gamma_c^{-2}\right) dy \tag{19}$$

Setting $n^2 - 1 - \gamma_c^{-2} = 0$ and inserting the expression for n (Eq. (16)) into Eq. (19), we get the Cerenkov line-width $\Delta\lambda_{\lim}^c$:

$$y_{\lim} \equiv \frac{\Delta\lambda_{\lim}^c}{\lambda_{lu}} = C_0 \gamma_c^2$$

$$= \frac{1}{16\pi^3 c} \lambda_{lu}^4 A_{ul} g_u \left(\frac{N_l}{g_l} - \frac{N_u}{g_u} \right) \gamma_c^2 \tag{20}$$

where

$$C_0 = \frac{1}{16\pi^3 c} \lambda_{lu}^4 A_{ul} g_u \left(\frac{N_l}{g_l} - \frac{N_u}{g_u} \right)$$

The Cerenkov radiation will be cut off at the wavelength displacement $\Delta\lambda_{\lim}^c$. Inserting Eqs. (16) and (20) into Eq. (19), the spectral emissivity becomes:

$$J_y^c dy = C_1 N_e \left(y^{-1} - y_{\lim}^{-1} \right) dy \tag{21}$$

where

$$C_1 \equiv \frac{e^2}{16\pi^2} \lambda_{lu}^2 A_{ul} g_u \left(\frac{N_l}{g_l} - \frac{N_u}{g_u} \right)$$

It is obvious that the emissivity $J_y^c = 0$, when $y = y_{\lim}$ (or $\Delta\lambda = \Delta\lambda_{\lim}^c$). But for small wavelength displacement $\Delta\lambda$, $y \ll y_{\lim}$, we have $J_y^c dy \propto y^{-1} \propto \Delta\lambda^{-1}$, i.e. J_y^c decreases with $\Delta\lambda$ slowly as $J_y^c \propto \Delta\lambda^{-1}$. Therefore, in the actual effective emission range $y \ll y_{\lim}$, we have a good approximation of Eq. (21)

$$J_y^c dy = C_1 N_e y^{-1} dy \tag{22}$$

We point out that there is a remarkable difference between the Cerenkov line emission and the usual spontaneous radiation transition, the later is determined by the population density in the upper level u, $J^s \propto N_u$. But the Cerenkov emissivity is determined by the difference in populations between the lower and upper levels $\left(\frac{N_l}{g_l} - \frac{N_u}{g_u} \right)$.

The original profile of the Cerenkov line is given by the calculated curve $J_y^c \sim y$ ($or J_\epsilon^c \sim \Delta\epsilon, or J_\lambda^c \sim \Delta\lambda$), as shown in Fig. 3a which is obtained from Eq. (22). However, for the small wavelength displacement $\Delta\lambda \simeq 0$, i.e. λ is very close to λ_{lu}, the approximate Eq. (22) has to be replaced by the strict Eq. (11) and Eq. (17).

2.2.2. Extended formulae of J_y^c and y_{lim}^c for complex atoms(ions) or molecules gas

The basic formulae for Cerenkov spectral emissivity J_y^c and maximum line-width y_{lim}, Eq. (20), Eq. (21) and Eq. (22) can be easily extended to the multi-electron complex atoms(ions) or molecular gas by use of the same simple replacement given by Eq. (5′) in Sect. 2.1.2, i.e. $N_l \rightarrow NS_l$, $N_u \rightarrow NS_u$. This is sufficient for the Cerenkov line of complex atoms in the optical band. However, if the Cerenkov line is located in the X-ray band, e.g. the Cerenkov Fe K_α line at ~ 6.4KeV, it is more convenient to replace the wavelength λ in Eqs. (20), (21) and (22) by the photon energy $\epsilon = h\nu$, $\lambda_{lu} \rightarrow \epsilon_{lu} = \frac{hc}{\lambda_{lu}}$. This is easy to do because of the simple relation $J_\lambda^c d\lambda = J_y^c dy = J_\epsilon^c d\epsilon$ and $y = \frac{\lambda - \lambda_{lu}}{\lambda_{lu}} = \frac{\nu_{lu} - \nu}{\nu_{lu}} = \frac{\epsilon_{lu} - \epsilon}{\epsilon_{lu}}$. Therefore, the Cerenkov spectral emissivity and line-width of complex atoms in X-ray band are still given by Eq. (20), (21) and (22) respectively, but the parameters are changed as

$$C_0 \equiv \frac{c^3 h^4}{16\pi^3} \epsilon_{lu}^{-4} A_{ul} g_u N \left(\frac{S_l}{g_l} - \frac{S_u}{g_u} \right) \tag{20'}$$

and

$$C_1 \equiv \frac{e^2 c^2 h^2}{16\pi^2} \epsilon_{lu}^{-2} A_{ul} g_u N \left(\frac{S_l}{g_l} - \frac{S_u}{g_u} \right) \tag{21'}$$

We emphasize again that $\epsilon_{lu} = \epsilon_u - \epsilon_l$ in Eq. (20′) and (21′) is in unit of ergs in CGSE system, rather than in KeV as usually used in the X-ray astronomy.

2.3. The absorption coefficient

2.3.1. Formulae for hydrogen and hydrogen-like gas

For an optically thick dense gas for which the Cerenkov line mechanism is efficient, the final emergent intensity I_λ^c is determined by the competition between the emission J_λ^c and the absorption k_λ. Therefore it is necessary to consider the absorption of the gas at $\lambda \simeq \lambda_{lu}$. For the optical and X-ray wavebands, there are two main absorption mechanisms that are relevant to the Cerenkov line emission. One is the line absorption k_{lu} in the vicinities of atomic lines, directly related to the extinction coefficient κ given in Eqs. (11) and (16) by the relation $k_{lu} = 4\pi\kappa/\lambda$.
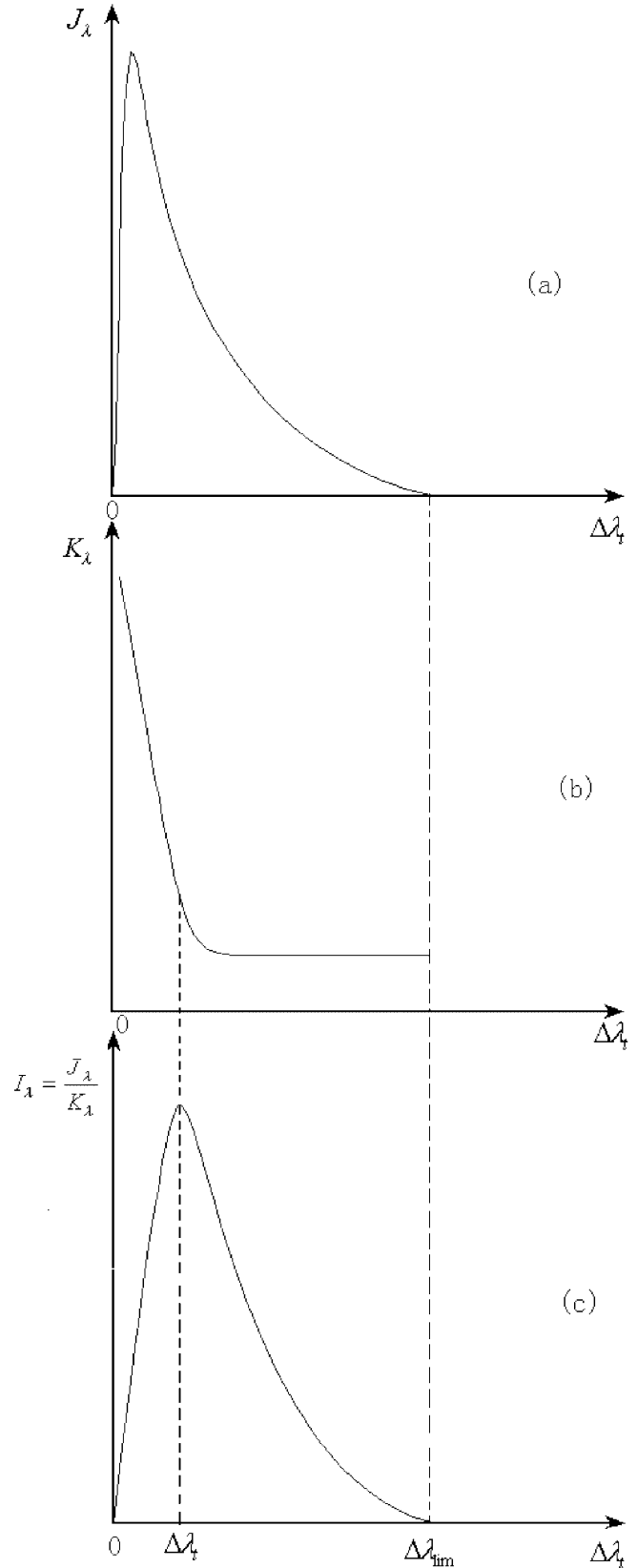
Fig. 3a–c. The Cerenkov emissivity J_λ **a**, absorption coefficient k_λ **b**, and the emergent intensity I_λ of the Cerenkov line (optically thick case) **c**. From **c** we see, the Cerenkov linewidth is large. The line profile is asymmetric with a small redshift.

Another is the photoelectric absorption k_{bf}, the free-free absorption k_{ff} is very small in the optical or X-ray band in which we are mainly interested, and can be neglected. Thus, for us, in the dust-free case, the total absorption is:

$$k = k_{lu} + k_{bf} \qquad (23)$$

k_{lu} can be obtained from the well known formula in molecular optics, $k_{lu} = \frac{4\pi}{\lambda}\kappa_\lambda = \frac{4\pi}{\lambda_{lu}}(1-y)\kappa_\lambda \simeq \frac{4\pi}{\lambda_{lu}}\kappa_\lambda$. Using Eq. (16) and retaining the lowest order of y, we have:

$$k_{lu} = \frac{1}{32\pi^3 c^2}\lambda_{lu}^4 A_{ul}\Gamma_{lu}g_u\left(\frac{N_l}{g_l} - \frac{N_u}{g_u}\right)y^{-2} = C_2 y^{-2} \quad (24)$$

where

$$C_2 \equiv \frac{1}{32\pi^3 c^2}\lambda_{lu}^4 A_{ul}\Gamma_{lu}g_u\left(\frac{N_l}{g_l} - \frac{N_u}{g_u}\right)$$

Therefore the resonance absorption $k_{lu} \propto \Delta\lambda^{-2}$ decreases rapidly with $\Delta\lambda$.

Here, we point out that k_{lu} can be obtained in another way which is more familiar to astronomers. The well known formula for line absorption is:

$$k_{lu} = \frac{c^2 N_l}{8\pi\nu^2}\left(\frac{g_u}{g_l}\right)\left(1 - \frac{g_l N_u}{g_u N_l}\right)A_{ul}\varphi_{ul}(\nu)$$

where, $\varphi_{ul}(\nu)$ is the Lorentz profile factor

$$\varphi_{ul}(\nu) = \frac{\Gamma_{lu}/4\pi^2}{(\nu - \nu_{lu})^2 + (\Gamma_{lu}/4\pi)^2} \simeq \frac{\Gamma_{lu}}{4\pi^2(\nu - \nu_{lu})^2}$$

Combining these two expressions, we obtain Eq. (24) again.

The photoionization absorption coefficient is $k_{bf} = \sum_s N_s\sigma_{bf}(s)$, where the summation extends over all levels for which the photoionization potential is less than incident photon energy $h\nu$, $I_s \leq h\nu$. In normal astrophysical conditions, the most important photoionization absorber is the neutral hydrogen due to its great abundance. Therefore, in optical wavebands we only consider the absorption by neutral hydrogen in the calculation of k_{bf} (H_e is the next candidate in the detailed calculation). The photoelectric cross section of level s of the hydrogen atoms is:

$$\sigma_{bf}(s) = 2.8 \times 10^{29}\nu^{-3}s^{-5}$$

or

$$\sigma_{bf}(s) = 1.04 \times 10^{-2}s^{-5}\lambda_{lu}^3(1+y)^3 \simeq 1.04 \times 10^{-2}s^{-5}\lambda_{lu}^3$$

(we keep the lowest order of y) Therefore

$$k_{bf} \simeq 1.04 \times 10^{-2}\lambda_{lu}^3\sum_{s\geq p} N_{H_s^0}s^{-5}$$

$$\simeq 1.04 \times 10^{-2}\lambda_{lu}^3 N_{H_p^0}p^{-5} \qquad (25)$$

The last approximation step in Eq. (25) means that only the absorption of the lowest photoelectric level $s = p$ (i.e. the largest term in the summation) is taken into consideration. The calculated $k_\lambda = k_{lu} + k_{bf} \sim \Delta\lambda$ curve is shown in Fig. 3b. Comparing Eq. (25) with Eq. (24), we see that the line absorption

$k_{lu} \propto y^{-2}$ decreases rapidly with increasing y, so k_{lu} is effective only in a very narrow range near to λ_{lu}, while the photoelectric absorption k_{bf} is nearly independent of wavelength displacement $\Delta\lambda$ (or y). Over the whole width of the Cerenkov line, k_{bf} is actually the main absorption that determines the integrated emergent intensity. The main effect of k_{lu} is to shift the line towards the red side of λ_{lu} (i.e. the Cerenkov line redshift).

2.3.2. Extended formulae of absorption k for complex atoms(ions) gas

As for the complex atoms(ions), the absorption coefficient k is still given by Eq. (23), where the line absorption k_{lu} is still given by Eq. (24), $k_{lu} = C_2 y^{-2}$. But the parameter C_2 is expressed as

$$C_2 \equiv \frac{1}{32\pi^3 c^2}\lambda_{lu}^4 A_{ul}\Gamma_{ul}g_u N\left(\frac{S_l}{g_l} - \frac{S_u}{g_u}\right) \qquad (24')$$

i.e. we use the replacement $N_l \rightarrow NS_l$, $N_u \rightarrow NS_u$, where N is the density of the multi-electron complex atoms concerned. Futhermore, if the Cerenkov line is located in the X-ray band, C_2 is expressed as

$$C_2 \equiv \frac{c^2 h^4}{32\pi^3}\epsilon_{lu}^{-4} A_{ul}\Gamma_{ul}g_u N\left(\frac{S_l}{g_l} - \frac{S_u}{g_u}\right) \qquad (24'')$$

where ϵ_{lu} is in ergs. i.e. we have used the replacement $\lambda_{lu} = \frac{hc}{\epsilon_{lu}}$ in Eq. (24') to get (24'').

However, when the Cerenkov line is in the X-ray band, we must take care for the calculation of the second kind of absorption, the photoionization k_{bf}, because of the fact that the hydrogen is no longer an important species responsible for the photoelectric absorption due to its very small photoelectric absorption cross section in the X-ray band ($\sigma_{bf} \propto \nu^{-3}$, see Eq. (25)), in spite of the great abundance of hydrogen in cosmological plasma.

In fact, for a given emission line in the X-ray band, the dominant contributors to the photoelectric absorption are the heavy elements with high Z, including the relevant multi-electron atom itself, which produces the emission line concerned (see the frequency behaviour of the photoelectric absorption cross section shown in Eq. (26) below, which shows the cross section σ_{bf} reaches a maximum at each absorption edge of the given atom, then decreases drastically as $\propto \nu^{-3}$). For example, for Fe K_α line at ~ 6.4KeV, the dominant photoionization absorbers are approximately the iron atoms or ions themselves, rather than other elements, Ca, O, S, etc., due to the highest abundance of Fe among the heavy elements with high Z. Furthermore, the main energy levels of the electron of the complex atom which are responsible for the photoelectric absorption are the K, L, M shells of the heavy elements. For example, for Fe K_α line ~ 6.4KeV, the most important contributors to the photoelctric absorption are the electrons in L shell of Fe ions. The ionization potential of the Fe K-shell is $I_K \sim 7.2$KeV, higher than 6.4KeV. Thus the electrons in the K-shell of the iron atom or ions can not be photoionized by the incident Fe K_α photons

~ 6.4KeV. Therefore, for Fe K_α line, we have

$$k_{bf} = \sum_{s \geq 2} N(Fe) S_s \sigma_{bf}(s) \simeq N(Fe) S_2 \sigma_{bf}(2) \qquad (25')$$

where $N(Fe)$ is the density of Fe in the gas, S_2 is the occupation number of electrons at $s = 2$ energy level, $S_2 \leq g_2$, $\sigma_{bf}(2)$ is the photoelectric cross section of an electron at $s = 2$ level. The last approximation in $(25')$ means that we only keep the largest term in the summation due to the fact that $\sigma_{bf}(2)$ is the largest one around ~ 6.4KeV, comparing with $\sigma_{bf}(3)$, $\sigma_{bf}(4)$ $\cdots$, i.e. $\sigma_{bf}(2) \gg \sigma_{bf}(3) \gg \sigma_{bf}(4)$. For the Fe atom and/or ions, the hydrogen-like formula for the cross section is a good approximation, particularly for the low-lying levels $s = 2, 3$

$$\sigma_{bf}(\nu, s) = \frac{32\pi^2 e^6 R_\infty Z^4}{3\sqrt{3} h^3 \nu^3 s^5} g_{fb}(\nu, T) \qquad (26)$$

Therefore $\sigma_{bf}(2)$ in Eq. $(25')$ is (taking $Z^{eff.} = 24$ for $s = 2$ level, i.e. for electron in the L-shell, the effective $Z^{eff.} = 24$)

$$\sigma_{bf}(2) \simeq 2.9 \times 10^{33}/\nu^3 \simeq 2.9 \times 10^{33}/\nu_{lu}^3 \ \ (\text{cm}^2)$$

Inserting to Eq. $(25')$, we get

$$k_{bf} = 8.4 \times 10^{-46} N(Fe) S_2 \epsilon_{lu}^{-3} \qquad (25'')$$

where $\epsilon_{lu} \equiv \epsilon_{21} = 6.4$KeV $= 1.025 \times 10^{-8}$(ergs) in unit ergs.

2.4. The emergent spectral intensity I_λ^c (or I_y^c). The line profile

In this section, we present formulae describing the Cerenkov intensity and the line profile, emergent from a plane-parallel emission slab. Similarly, we first discuss the hydrogen or hydrogen-like gas. Using the J_y^c and k_y given above, the emergent Cerenkov line intensity I_λ^c from the surface of the slab can be calculated by the equation of radiative transfer:

$$\frac{d}{d\tau_\lambda}\left[\frac{I_\lambda^c(x)}{n_\lambda^2}\right] = S_\lambda - \frac{I_\lambda^c(x)}{n_\lambda^2} \qquad (27)$$

where, $d\tau_\lambda = k_\lambda ds$ is the elementary optical depth, $S_\lambda \equiv J_\lambda^c/k_\lambda n_\lambda^2$ is the source function.

2.4.1. I_λ^c (or I_y^c) and the line profile
of the Cerenkov line of hydrogen or hydrogen-like gas

Case A. The uniform plane-parallel slab. For a uniform plane-parallel slab of an emitting gas with thickness L, the solution of Eq. (27) gives the emergent spectral intensity I_λ^c:

$$I_\lambda^c = n_\lambda^2 S_\lambda (1 - e^{-\tau_\lambda}) = \frac{J_\lambda^c}{k_\lambda}\left(1 - e^{-k_\lambda L}\right) \qquad (28)$$

where $k_\lambda L = \tau_\lambda$ is the optical thickness of the uniform slab of the emission gas. Replacing λ by $y \equiv \Delta\lambda/\lambda_{lu}$, Eq. (28) can be expressed in an equivalent form:

$$I_y^c = \frac{J_y^c}{k_y}\left(1 - e^{-k_y L}\right) \qquad (29)$$

However, we shall be particularly interested in the optically thick case, because our main interest is in the high energy astrophysical objects, such as QSOs, supernovae, solar flares, etc., and we know that these objects all have compact structures in which the gas density is high, and near the optically thick case. On the other hand, in Sec. 1, we have argued that the Cerenkov line radiation becomes important only when the gas is dense and optically thick for continuum, i.e. $k_\lambda L = (k_{lu} + k_{bf})L \gg 1$. In the optically thick case, Eq. (29) becomes $I_y^c = J_y^c/k_y$ or

$$I_\lambda^c \simeq J_\lambda^c/k_\lambda \qquad (30)$$

where, J_λ^c, $k_\lambda = k_{lu} + k_{bf}$ have been given in Eqs. (21), (24) and (25), in which the variable is $y = \Delta\lambda/\lambda_{lu}$, rather than $\Delta\lambda$. Therefore Eq. (30) becomes:

$$I_y^c = \frac{J_y^c}{k_{lu} + k_{bf}} = \frac{N_e C_1 \left(y^{-1} - y_{\lim}^{-1}\right)}{C_2 y^{-2} + k_{bf}} \qquad (31)$$

where, C_1, C_2 and k_{bf} are given in Eqs. (21), (24) and (25) respectively, and $y_{\lim}^c = C_0 \gamma_c^2$, C_0 is given in Eq. (20).

For convenience, we re-list the constants as follows:

$$
\begin{aligned}
C_0 &= \frac{1}{16\pi^3 c}\lambda_{lu}^4 A_{ul} g_u \left(\frac{N_l}{g_l} - \frac{N_u}{g_u}\right) \\
&\simeq 6.72 \times 10^{-14} \lambda_{lu}^4 A_{ul} \frac{g_u}{g_l} N R_l \\
C_1 &= \frac{e^2}{16\pi^2}\lambda_{lu}^2 A_{ul} g_u \left(\frac{N_l}{g_l} - \frac{N_u}{g_u}\right) \\
&\simeq 1.46 \times 10^{-21} \lambda_{lu}^2 A_{ul} \frac{g_u}{g_l} N R_l \\
C_2 &= \frac{1}{32\pi^3 c^2}\lambda_{lu}^4 A_{lu} \Gamma_{lu} g_u \left(\frac{N_l}{g_l} - \frac{N_u}{g_u}\right) \\
&\simeq 1.12 \times 10^{-24} \lambda_{lu}^4 A_{ul} \Gamma_{lu} \frac{g_u}{g_l} N R_l \\
k_{bf} &= 1.04 \times 10^{-2} \lambda_{lu}^3 N_{H_p^0} p^{-5} \\
&= 1.04 \times 10^{-2} \lambda_{lu}^3 N_{H^0} p^{-5} R_p
\end{aligned}
\qquad (32)
$$

(Note that the wavelength λ_{lu} in Eqs. (32) is in centimeter rather than Å)

The last step approximation in Eqs. (32) is due to the fact that, in the normal conditions of a gaseous medium, at least for the lowest levels, we have $N \simeq N_1 \gg N_2 \gg N_3 \cdots$, or $N_l \gg N_u$. So $\left(\frac{N_l}{g_l} - \frac{N_u}{g_u}\right) \simeq \frac{N_l}{g_l} = \frac{1}{g_l} R_l N$, N is the total density of the hydrogen or hydrogenic atom (or ion) species concerned, e.g. $N = N(Mg^+)$, N_{H^0}, $N(Na^0) \cdots$ for the calculation of Cerenkov lines of $MgII, HI, NaI, \cdots$. $R_l \equiv \frac{N_l}{N}$ is the fractional population in the level l of the concerned atom (ion) species. Similarly, $\sum_{s \geq p} N_{H_s^0} s^{-5} \simeq R_p N_{H^0} p^{-5}$, where N_{H^0} is the number density of the neutral hydrogen atom in the uniform slab, $R_p \equiv N_{H_p^0}/N_{H^0}$ is the fractional population of the neutral hydrogen in the lowest photoelectric level p.

Finally, for comparison with the observations, it is necessary to transform I_y^c in Eq. (31) into I_λ^c. Using $I_y^c dy = I_\lambda^c d\lambda$ and $dy = \frac{1}{\lambda_{lu}} d\lambda$, we have:

$$I_\lambda^c = \frac{1}{\lambda_{lu}} I_y^c \qquad (33)$$

If the conventional unit $(\text{ergs}/\text{cm}^2 \cdot \text{sec} \cdot \text{str} \cdot \text{Å})$ is adopted for I_λ^c, then Eq. (33) becomes $I_\lambda^c = \frac{10^{-8}}{\lambda_{lu}} I_y^c$. By use of Eqs. (31), (32) and (33), the calculated profile of the Cerenkov line $I_\lambda^c \sim \Delta\lambda$ in the optically thick case is shown in Fig. 3c, which is broad (line-width $\Delta\lambda_{\lim} = \lambda_{lu} y_{\lim} = C_0 \lambda_{lu} \gamma_c^2$); slightly red shifted; and red-asymmetric, as mentioned above. Here we emphasized that the formula of spectral intensity Eq. (31) is obtained by the use of the approximate formulae Eqs. (16), (21) and (24), which are valid only if the condition (14), e.g. $g \ll z, b \ll z$, is satisfied (That is, the fractional wavelength displacement y cannot be indefinitely small, $y \equiv \frac{\Delta\lambda}{\lambda_{lu}} \nrightarrow 0$. Otherwise $J_y^c \propto y^{-1} \to \infty$ and $k_{lu} \propto y^{-2} \to \infty$, which are obviously unacceptable). However, the derived formula of I_y^c, i.e. Eq. (31) can be safely extended to $y \to 0$ without any divergence. Particularly we have $I_y^c = 0$ at $y = 0$. Therefore, Eq. (31) is valid in the whole waveband of the Cerenkov line $(0, y_{\lim})$.

Case B. The non-uniform plane-parallel slab. For a non-uniform plane-parallel slab of emissive gas, Eq. (28), and hence Eqs. (29)–(31) are no longer valid. In this case, the solution of the equation of radiative transfer Eq. (27) will take the original form: $\frac{I_\lambda^c}{n_\lambda^2} = \int_0^{\tau_\lambda(L)} e^{-\tau_\lambda} \left(\frac{J_\lambda^c}{n_\lambda^2 k_\lambda} \right) d\tau_\lambda$. But we have pointed out that in the effecting Cerenkov emission range, the actual index $n_\lambda \simeq 1$. Therefore we have:

$$I_\lambda^c = \int_0^{\tau_\lambda(L)} e^{-\tau_\lambda} \left(\frac{J_\lambda^c}{k_\lambda} \right) d\tau_\lambda \tag{34}$$

In the non-uniform case, the factor $(J_\lambda^c / k_\lambda)$ can not be taken outside the integral, because it is dependent on the position s, $J_\lambda^c \propto N_l = N_l(s)$ and $k_\lambda \simeq k_{bf} \propto N_{H^0} = N_{H^0}(s)$, and so is the ratio $(J_\lambda^c / k_\lambda)$. Therefore Eq. (34) can not be simplified to Eq. (28) (but neutral hydrogen is an exception, for H^0, $J_\lambda^c \propto N_{H_l^0}(s)$ and $k_\lambda \simeq k_{bf} \propto N_{H^0}(s)$, the ratio J_λ^c / k_λ is s-independent, therefore Eq. (28)–(31) are still valid for hydrogen despite of the drastic nonuniform variation of $N_{H^0}(s)$ near the front H^+ / H^0). Eq. (34) can be re-written as:

$$I_\lambda^c(L) = \int_0^L J_\lambda^c(s) e^{-\int_0^s k_\lambda(s')ds'} ds \tag{35}$$

If the effective interval where $J_\lambda^c(s) \neq 0$ is (S_1, S_2) rather than $(0, L)$, then Eq. (35) can be rewritten as:

$$I_\lambda^c = \int_{S_1}^{S_2} J_\lambda^c(s) e^{-\int_0^s k_\lambda(s')ds'} ds \tag{36}$$

Eq. (36) gives the emergent spectral intensity of the nonuniform plan-parallel slab. The integral can be evaluated numerically if $J_\lambda^c(s)$ and $k_\lambda(s)$ are given at each point s along the ray. However, in some cases, a semi-quantitative estimation of I_λ^c is good enough. We suggest a simple expression with a similar form of Eq. (30) for the uniform case, to replace Eq. (36):

$$I_\lambda^c = \frac{\overline{J_\lambda^c}}{\overline{k_\lambda}} = \frac{\int_{S_1}^{S_2} J_\lambda^c(s)ds}{\int_{S_1}^{S_2} k_\lambda(s)ds} \tag{37}$$
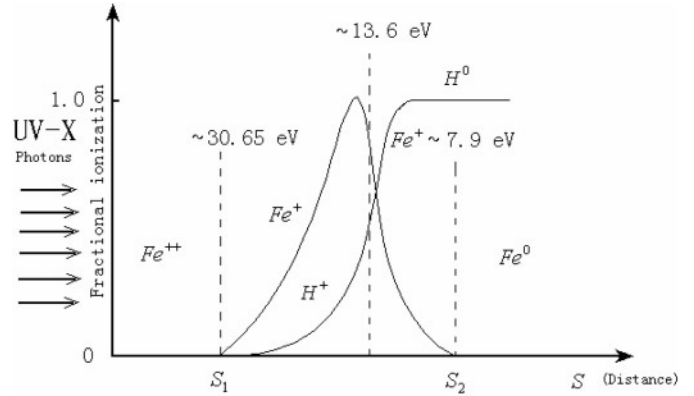
Fig. 4. The schematic distributions of Fe^+ and H^0 near the H^+ / H^0 ionization front, i.e. the ionization structure of the surface layer of the cloud in BLR.

where, the integral region (S_1, S_2) expresses the range where the atom (or ion) species concerned exists, hence $J_\lambda^c(s) \neq 0$, and $k_\lambda(s) \neq 0$.

The special importance of the non-uniform plane-parallel slab is in that, according to the conventional photoionization model of BLR of AGNs, most low-ionized ions particularly the hydrogenic ions, e.g. $Fe^+, Mg^+, \cdots$, exist in a layer near to the ionization front of H^+ / H^0, and have a non-uniform distribution, $N_{Fe^+} = N_{Fe^+}(s)$, $N_{Mg^+} = N_{Mg^+}(s), \cdots$. For example, it is known that the ionization thresholds of iron are $Fe^0 / Fe^+ / Fe^{++} = 7.9/16.18/30.65 \text{eV}$, and the position of the front H^+ / H^0 is at $\sim 13.6 \text{eV}$. So we infer that the low-ionized ions Fe^+ exist on both sides of the front H^+ / H^0, where the density of neutral hydrogen N_{H^0} varies drastically with s, $N_{H^0} = N_{H^0}(s)$, the same as the density of Fe^+, $N_{Fe^+} = N_{Fe^+}(s)$. Fig. 4 shows the schematic distribution of Fe^+, H^0, H^+, in the neighbourhood of the front of $H^+ / H^0 \sim 13.6 \text{eV}$.

2.4.2. Extended formulae of intensity I_y^c for complex atoms(ions) gas

For simplicity, we only give the formulae for the uniform and optically thick plane-parallel emission slab. The discussion is parallel to Sect. 2.4.1 for the hydrogenic atoms. Thus Eq. (31) is still valid for the heavy elements, only with a replacement of $N_l \to NS_l$ and $N_u \to NS_u$ (Eq. (5') in the expressions of C_0, C_1, C_2 in Eqs. (32), we then get the emergent intensity I and the line profile for the Cerenkov line of the complex atoms(ions). Furthermore, in the optical waveband, the dominant absorber of photoionization is still hydrogen due to the great abundance of H, thus k_{bf} is still given by the last equation in Eqs. (32).

However, if the Cerenkov line is located in the X-ray waveband, e.g. the Cerenkov Fe K_α line $\sim 6.4 \text{KeV}$, we must use the parameters C_0, C_1, C_2 and k_{bf} given by Eq. (20'), (21'), (24'') and (25'), (25'') respectively. For convenience, we relist all of these parameters in Eq. (32') below. Therefore, in Eq. (31),

$$y = \frac{\epsilon_{lu} - \epsilon}{\epsilon_{lu}}$$

$$C_0 = 1.05 \times 10^{-76} \epsilon_{lu}^{-4} A_{ul} g_u N \left(\frac{S_l}{g_l} - \frac{S_u}{g_u} \right)$$

$$C_1 = 5.77 \times 10^{-53} \epsilon_{lu}^{-2} A_{ul} g_u N \left(\frac{S_l}{g_l} - \frac{S_u}{g_u} \right)$$

$$C_2 = 1.75 \times 10^{-87} \epsilon_{lu}^{-4} A_{ul} \Gamma_{lu} g_u N \left(\frac{S_l}{g_l} - \frac{S_u}{g_u} \right)$$

$$k_{bf} = 8.4 \times 10^{-46} \epsilon_{lu}^{-3} N(Fe) S_2 \quad (\text{for } Fe\ K_\alpha - \text{line}) \quad (32')$$

and ϵ_{lu} is in unit ergs in CGSE system ($1 \text{KeV} = 1.602 \times 10^{-9}$ erg).

Using Eq. (31), we calculated the Cerenkov K_α line $\sim$ 6.4KeV of the iron ion Fe^{+19}, as shown in Fig. 5. The calculation parameters are chosen as $\gamma_c = 1.0 \times 10^4$, $N = 2.5 \times 10^{19} \text{cm}^{-3}$ (Fig. 5a) and $\gamma_c = 1.0 \times 10^4$, $N = 2.5 \times 10^{17} \text{cm}^{-3}$ (Fig. 5b) respectively.

2.5. The Cerenkov line redshift y_t^c (or ΔZ^c)

2.5.1. Formulae of y_t^c (or ΔZ^c)
for hydrogen or hydrogen-like gas

Using Eq. (31), the small "Cerenkov line redshift" y_t^c can be obtained from the equation $\frac{dI_y^c}{dy} = 0$. Thus we obtained:

$$\Delta Z^c \equiv y_t^c = \frac{\Delta \lambda_t^c}{\lambda_{lu}} = \frac{1}{y_{\lim}^{-1} + \sqrt{y_{\lim}^{-2} + \frac{k_{bf}}{C_2}}}$$

$$= \frac{1}{C_0^{-1} \gamma_c^{-2} + \sqrt{C_0^{-2} \gamma_c^{-4} + \frac{k_{bf}}{C_2}}} \quad (38)$$

If the gas is very dense (e.g. $N_{H^0} \simeq 10^{16} \text{cm}^{-3}$), we have a line width $y_{\lim} \gg \sqrt{C_2/k_{bf}}$ ($y_{\lim} \equiv \frac{\Delta \lambda_{\lim}^c}{\lambda_{lu}} \propto C_0 \propto N$, but C_2/k_{bf} is density-independent, see Eqs. (20), (32). Therefore from Eqs. (32) and (38) we get a simplified redshift formula:

$$\Delta Z^c \equiv y_t^c \simeq \sqrt{\frac{C_2}{k_{bf}}}$$

$$= 1.04 \times 10^{-11} \sqrt{\lambda_{lu} A_{ul} \Gamma_{lu} \frac{g_u}{g_l} R_l R_p^{-1} p^5 \xi} \quad (39)$$

where $\xi \equiv N/N_{H^0}$ represents the "abundance" of the concerned hydrogenic atom (ions) species. For the gas of neutral hydrogen $\xi = 1$. It is easy to show that the wavelength displacement y_t^c in Eq. (39) is just at the wavelength position where $k_{lu} = k_{bf}$. For the wavelength region $y \le y_t^c$ which is close to λ_{lu}, we have $k_{lu} \gg k_{bf}$ which means that the Cerenkov line redshift is just caused by the great line absorption k_{lu} at vicinity of λ_{lu}. From Eq. (39) we see, the redshift for the dense gas is N-independent, ΔZ^c is only dependent on the atomic parameters ($\lambda_{lu}, A_{ul}, \Gamma_{lu}, \cdots$) and the temperature T of the gas, and the "abundance" $\xi \equiv N/N_{H^0}$.

Another limiting case is for the gas with lower density, which makes $y_{\lim} \ll \sqrt{\frac{C_2}{k_{bf}}}$. In this case (but still optically thick for

(a)

(b)

(c)
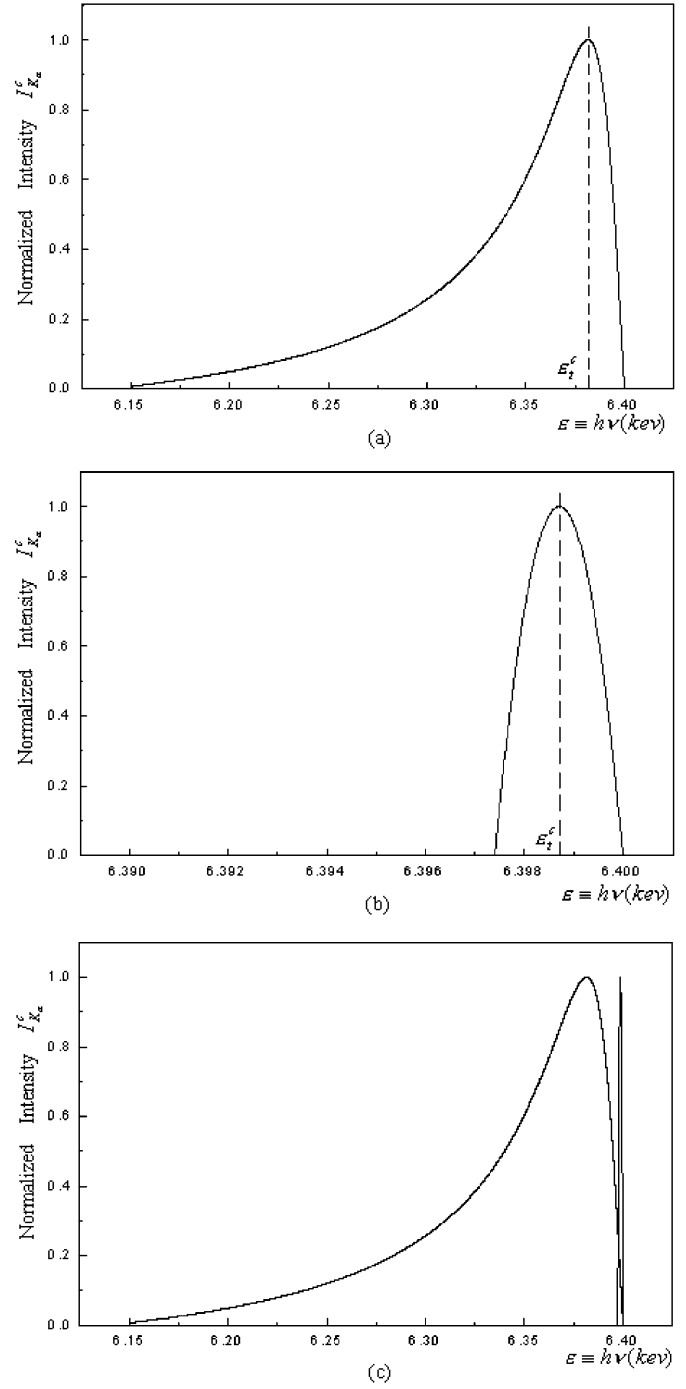
Fig. 5a–c. The emergent intensity I_λ^c of Fe^{+19} ions. **a** shows the line profile of Fe^{+19} in gas of higher density $\gamma_c = 1.0 \times 10^4$, $N = 2.5 \times 10^{19}$; **b** shows a symmetric profile in gas of lower density $\gamma_c = 1.0 \times 10^4$, $N = 2.5 \times 10^{17}$; **c** combines the line-profiles of **a** and **b** for comparason.

continuum, $k_\lambda L = (k_{lu} + k_{bf})L \gg 1$)), Eq. (38) is simplified as:

$$\Delta Z^c \equiv y_t^c \equiv \frac{\Delta \lambda_t^c}{\lambda_{lu}} \simeq \frac{y_{\lim}}{2} \quad (40)$$

where, $y_{\lim}$ is given by Eq. (20) ($y_{\lim} \propto N$). The critical point of "higher" and "lower" densities is determined by a critical equality $y_{\lim} = \sqrt{\frac{C_2}{k_{bf}}}$, from which we get a critical density $N^{cr\cdot}$ of the concerned species in a gas:

$$N^{cr\cdot} = 1.54 \times 10^2 \left(\frac{g_u}{g_l}\right)^{-1/2}$$
$$\times \gamma_c^{-2} \lambda_{lu}^{-7/2} A_{ul}^{-1/2} \Gamma_{lu}^{1/2} p^{5/2} (R_l R_p)^{-1/2} \xi^{1/2} \qquad (41)$$

Therefore, Eq. (39) and Eq. (40) are valid for $N \gg N^{cr\cdot}$ and $N \ll N^{cr\cdot}$ respectively. Fig. 3c shows the profile $I_\lambda^c \sim \Delta\lambda$ and the redshift $\Delta\lambda^c$ of the Cerenkov line for the case $N \gg N^{cr\cdot}$. The red-asymmetry of the profile is remarkable. But for the cases $N \simeq N^{cr\cdot}$ and $N \ll N^{cr\cdot}$ (see Fig. 5b), the profile becomes more symmetric. And the Cerenkov line redshift becomes very small.

We emphasize again, both Eq. (39) for $N \gg N^{cr\cdot}$ and Eq. (40) for $N \ll N^{cr\cdot}$ are derived from Eq. (31). Both Eq. (39) and Eq. (40) are valid only for the optically thick case, $\tau_\lambda = (k_{lu} + k_{bf})L \gg 1$.

2.5.2. Extended formulae of y_t^c (or ΔZ^c) for complex atoms (ions) gas

The formula of the Cerenkov line redshift, Eq. (38) is also valid for a gas composed of complex atoms (ions). The related parameters in (38), i.e. C_0, C_1, C_2 and k_{bf} are still given by Eq. (32) only with replacement $\left(\frac{N_l}{g_l} - \frac{N_u}{g_u}\right) \Longrightarrow N\left(\frac{S_l}{g_l} - \frac{S_u}{g_u}\right)$, or equivalently, $N_l \to NS_l$, $N_u \to NS_u$ (see Eq. (5″)), with unchanged k_{bf} because the dominant photoionization absorber in the optical wavelength is still hydrogen.

In parallel, in the limiting cases, $y_{\lim} \gg \sqrt{\frac{C_2}{k_{bf}}}$ and $y_{\lim} \ll \sqrt{\frac{C_2}{k_{bf}}}$, or equivalently, $N \gg N^{cr\cdot}$ and $N \ll N^{cr\cdot}$, the simplified redshift formulae are still given by Eq. (39) and (40) respectively.

If the Cerenkov line of complex atoms or ions is in the X-ray band, it is better to change the wavelength in (32) into the photon energy, $\lambda_{lu} \to \epsilon_{lu}$, $\lambda_{lu} = \frac{hc}{\epsilon_{lu}}$, i.e. the parameters C_0, C_2 and k_{bf} in (38) have to be expressed by Eq. (32′). given in Sect. 2.4.2, where $\epsilon_{lu} \equiv \epsilon_u - \epsilon_l = h\nu_{lu}$ is in unit ergs in the CGSE system, rather than KeV (1KeV=1.602 $\times 10^{-9}$ergs).

2.6. The emergent intensity I^c of the Cerenkov line

2.6.1. Formulae of I^c for hydrogen of hydrogen-like gas

Integrating Eq. (31), we obtained the total intensity I^c of the Cerenkov line, for the optically thich uniform plane-parallel layer $I^c = \int_0^{y_{\lim}} I_y^c dy$ Thus

$$I^c = Y \left[\ln(1 + X^2) - 2\left(1 - \frac{\arctan X}{X}\right)\right] \qquad (42)$$

where, $Y \equiv \frac{N_e}{2}\frac{C_1}{k_{bf}}$, N_e is the density of relativistic electrons, $X \equiv \sqrt{\frac{k_{bf}}{C_2}} y_{\lim}$, C_0, C_1, C_2 and k_{bf} are given by Eq. (32), $y_{\lim}$ is given by Eq. (20).

Eq. (42) is in principle valid for a uniform plane-parallel slab of emissive gas. But as an exception, it can be used to calculate the line intensity of the neutral hydrogen without any problem. Although the density of H^0 atoms, N_{H^0} varies with depth s drastically near the front H^+/H^0, $N_{H^0} = N_{H^0}(s)$, we point out that the ratio $(J_\lambda^c/k_\lambda)_{H^0}$ is constant, despite the nonuniform ionization structure in the neighbourhood of the front H^+/H^0. Therefore $(J_\lambda^c/k_\lambda)_{H^0}$ can be taken out of the integral $I_\lambda^c = \int_0^{\tau_\lambda(u)} e^{-\tau_\lambda}\left(\frac{J_\lambda^c}{k_\lambda}\right)d\tau_\lambda \simeq \frac{J_\lambda^c}{k_\lambda}$, which ensures the validity of Eq. (42).

For the non-uniform case, the low-ionization line, such as $Mg^+, Fe^+, O^+, \cdots$, the emergent intensity of Cerenkov line I^c, is also obtained from $I^c = \int_0^{y_{\lim}} I_y^c dy$, and I_y^c is given by Eq. (35). The calculation is somewhat complicate. However, in the semi-quantitative estimation of I^c, we can still invoke Eq. (42) only regarding the factors $R_l \equiv N_l/N$, $R_p \equiv N_{H_p^0}/N_{H^0}$, particularly, $\xi \equiv N/N_{H^0}$ etc. as the average value $\overline{R_l}, \overline{R_p}, \overline{\xi}, \cdots$, in the interval (S_1, S_2), where the concerned atoms or ions exist.

2.6.2. Extended formulae of I^c for complex atoms (ions) gas

The emergent total intensity of the Cerenkov line of the complex atoms (ions) in the optically thick case is also given by Eq. (42), where C_0, C_1, C_2 and k_{bf} are given by Eq. (32) replacing N_l by NS_l and N_u by NS_u. Note that, when the Cerenkov line is in the X-ray band, Eq. (32′) has to be used to replace Eq. (32).

3. Conclusion and discussion

The Cerenkov line-like emission of the relativistic electrons, passing through an optically thick dense gas, which we suggested early in 1980, has been verified by elegant laboratory experiments (Xu et al. 1981, 1988, 1989). In this paper, we give a detailed and clearer physical discussion and emphasize the potential importance of this new mechanism for high-energy astrophysics, and give the extended and improved formula system describing the emergent intensity, the line profile, the line width and the Cerenkov redshift of the Cerenkov line, among which the extension of formulae to the multi-electron complex atoms(ions) has special significance for the study of the broad lines of heavy elements in AGNs, particularly for lines in the X-ray band.

A possible application of the new line emission mechanism is in the exploration of the origin of the broad ~ 6.4KeV K_α line of the low-ionized iron ions of Seyfert1 galaxies. Now the disk-line models, in which the ~ 6.4KeV K_α line is regarded as one of the reflection components from the disk, strongly illuminated by the hard X-ray continuum, are widely accepted to explain the origin and characters of the broad K_α-line with asymmetric profile. It is believed that the "Compton reflection and iron fluorescence features", provide a powerful probe of

the accretion flow and the strong gravitational field (see e.g. Georgy & Fabian 1991; Reynolds et al. 1995). However, people now question the relativistically smeared disk-line interpretation. According to the disk-line model, both the line profile and the position of the peak are dependent on the inclination angle θ of the disk, and therefore are different from one sample to another. But the observations show similar profiles of the K_α line for all Seyfert1 galaxies, even for Seyfert2 galaxies, with nearly unchanged peak at $\sim 6.4\text{KeV}$ (Nandra, 1997,a,b), which implies that the K_α line might not be from the inner disk, as thought before. It seems more reasonable to replace the "cold disk" by "cold cloudlets" and/or "cold filaments" around the central massive black hole. Furthermore, the line emission mechanism might not, or rather, not only be photoionization-fluorescence. The photoionization-fluorescence model predicts positive correlations of both the light curves and the fluxes between the K_α line and the X-ray continuum. But the observations do not confirm this (e.g. Lee et al. 1999). Besides, the prediction of a marked absorption dip at edge $> 7\text{KeV}$ which always accompanies the fluorescent $\sim 6.4\text{KeV}$ K_α line is also not confirmed by the observations (Young et al. 1998).

We have shown that fluorescence is not a 'unique' mechanism of the line-emission of the low-ionization iron in the X-ray band. Another line mechanism which can produce the $\sim 6.4\text{KeV}$ K_α line is the Cerenkov line-like emission, as described in this paper. For a very dense gas, optically thick for the continuum, the Cerenkov line becomes the unique emission line which can escape from the surface of the cloud of dense gas. The Cerenkov line will be strong to match the observation when the density of relativistic electrons in BLR is high enough. Therefore this kind of line emission might be a new possi-

ble mechanism to attack the 6.4KeV K_α problem of AGNs. We expect that some puzzles of K_α line of iron could be resolved in this way (e.g. the observed strange correlations of the light curves and the fluxes between the K_α line and X-ray continuum radiation), even though there remain a lot of problems to be solved.

References

Bethe H.A., Salpeter E.E., 1957, Encyclopedia of Physics, 35, 88
Cheng F.H., You J.H., Yan M., 1990, ApJ 358, 18
Georgy I.M., Fabian A.C., 1991, MNRAS 249, 352
Handbook of Physics, Condon E., Odishaw H., 1958, McGraw-Hill Company Inc., Chap. 6, 112
Lee J.C., Fabian A.C., Reynolds C.S., Brandt W.N., Iwasawa K., 1999, MNRAS 310, 973
Nandra K., George I.M., Mushotzky R.F. et al., 1997a, ApJ 476, 70
Nandra K., George I.M., Mushotzky R.F. et al., 1997b, ApJ 477, 602
Reynolds C.S., Fabian A.C., Inoue H., 1995, MNRAS 276, 1311
Tanaka Y., Nandra K., Fabian A.C., et al., 1995, Nat 375, 659
Turner T.J., George I.M., Nandra K. et al., 1997, ApJS 113, 23
Xu K.Z., Yang B.X., Xi F.Y., 1981, Phys. Lett. A86, 24
Xu K.Z., Yang B.X., Xi F.Y., 1988, Phys. Rev. A33, 2912
Xu K.Z., Yang B.X., Xi F.Y., 1989, Phys. Rev. A40, 5411
You J.H., Cheng F. H., 1980, Acta Phys. Sinica 29, 927
You H., Kiang T., Cheng F.H., Cheng F.Z., 1984, MNRAS, 211, 667
You J.H., Cheng F.H., 1987, ApJ, 332, 174
You J.H., Cheng F.H., Cheng F.Z., Kiang T., 1986, Phys. Rev. A34, 3015
Young A.J., Ross R.R., Fabian A.C., 1998, MNRAS 300, L11